Atomistic simulation studies of trapped hole bipolarons in $BaTiO_3$

1995 J. Phys.: Condens. Matter 7 327

(http://iopscience.iop.org/0953-8984/7/2/010)

J. Phys.: Condens. Matter 7 (1995) 327–337. Printed in the UK

Atomistic simulation studies of trapped hole bipolarons in $BaTiO_3$

H Donnerberg and A Birkholz
University of Osnabrück, FB Physik, D-49069 Osnabrück, Germany

Received 12 August 1994, in final form 7 October 1994

Abstract. Classical shell-model- and embedded-cluster-type calculations are employed in order to supply theoretical arguments in favour of hole bipolarons in $BaTiO_3$ which have recently been speculated to exist in this photorefractive material. Our investigations concern the geometrical structure of hole bipolarons trapped at acceptor defects, their spin state and hole ionization energies. In particular the embedded-cluster modelling studies, which explicitly include the local electronic defect structure, suggest the importance of lattice relaxation and electron correlation terms in order to stabilize diamagnetic O_2^{2-} molecules (bipolarons) in $BaTiO_3$. Our simulations show that hole bipolarons are predominantly bound at Ti-site acceptor defects. A trapping of bipolarons at Ba-site acceptors is in most cases unfavourable. Finally, by extrapolating our present results to the high-T_c superconducting oxides we qualitatively discuss the possible rôle of small hole (peroxy) bipolarons in these materials.

1. Introduction

Photorefractive oxide crystals ABO_3 with perovskite structure are known to be of considerable technological importance. Recent applications concern the development of electro-optical device elements [1, 2].

The photorefractive behaviour of oxide perovskites is intimately connected with crystal defects which are always generated during the crystal growth. In particular transition-metal impurities (predominantly iron) are known to play a leading rôle in this respect. In brief the basic physics underlying the photorefractive effect may be summarized as follows. Resulting from interfering light beams striking a photorefractive oxide specimen the crystal sample is exposed to light and dark regions. Suitable defect centres in the light region, possessing electronic states within the bandgap, are subject to illumination-induced charge-transfer reactions by means of which mobile charge carriers are created, which in the case of $BaTiO_3$ are predominantly holes. Via diffusion, bulk photovoltaic effects and/or drift in pyroelectrical fields [3] these charge carriers are transported into the dark regions where they are again trapped by defects. The space-charge field generated this way gives rise to a corresponding pattern in the refractive indices.

The illumination-induced charge-transfer processes can be investigated on a microscopic level by means of photoelectron-spin-resonance techniques (photo-ESR), i.e. by detection of ESR changes as a function of the wavelength of the illuminating light. In this way it has been found that light-induced charge-transfer reactions must involve defect centres which are invisible in photo-ESR experiments, see figure 1 (reproduced from [4]). The figure displays a correlation of the observed ESR intensities of paramagnetic defects with the wavelength Λ of the illuminating light. Holes created in the valence band by photoionization of Fe^{4+} are trapped by ESR-silent defect centres, called X in figure 1, and, thus, remain invisible

0953-8984/95/020327+11$19.50

in the wavelength range 650 nm $< \Lambda <$ 850 nm. Only for even smaller wavelengths is the formation of single-hole centres observed. Since the employed crystal samples were as grown, they are characterized by having a low-lying Fermi-energy level, a situation that *a priori* favours the formation of high-valence impurity states such as Fe^{4+}.

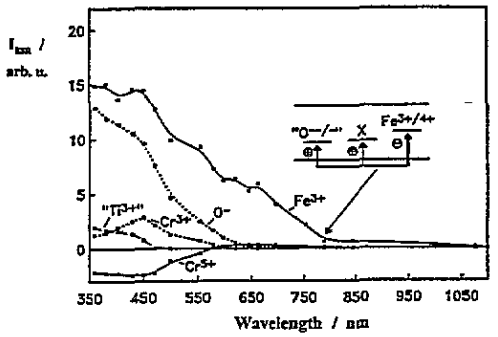

Figure 1. Typical photo-ESR spectrum obtained from as-grown $BaTiO_3$ specimen. Changes in the ESR intensity I_{ESR} are shown as a function of the wavelength of the illuminating light. The inset sketches the underlying dominating charge-transfer process. Diamagnetic centres X are speculated to correspond to diamagnetic hole bipolarons. The figure is reproduced from [4].

A reasonable explanation for the ESR-invisible hole centres has been given by Possenriede *et al* [4] which is based on hole-type bipolarons corresponding to molecular O_2^{2-} aggregates. Similar to isoelectronic F_2 molecules such oxygen complexes should possess a diamagnetic ground state, thus being insensitive to ESR. Nearby acceptor defects can be expected to aid the required hole localization. The onset wavelength of single-hole formation in figure 1 may then be interpreted as the light-induced dissociation of the bipolarons.

Since there is no direct experimental evidence giving hints at the nature of these ESR-silent defect centres, theoretical modelling studies should be valuable in order to clarify questions concerning the possible existence of hole bipolarons in $BaTiO_3$. In this contribution we present computer simulations of trapped hole bipolarons which are based on shell-model calculations and additional embedded-cluster investigations. These computational techniques have proved to give reliable information on stability, geometrical structure and energy levels of localized defect centres.

2. Methods and results

2.1. Shell-model calculations

Within a classical shell-model approach [5] each ion is represented by a massive core to which a shell (charge Y) is harmonically bound (harmonic spring constant k). The (free) electronic polarizability of the ions is given by

$$\alpha = \frac{Y^2}{k}. \tag{1}$$

Pair potentials are specified between different ionic components. Besides the long-range Coulomb potentials one needs to consider short-range interactions representing the repulsion

between the charge clouds of neighbouring crystal ions as well as attractive interionic electronic correlation terms and covalency. A common choice for the functional form of these short-range interactions is the Buckingham potential:

$$V(r) = A\exp(-r/\rho) - \frac{C}{r^6}. \tag{2}$$

The *a priori* unknown parameters Y, k, A, ρ and C can be determined according to empirical fitting procedures or theoretical schemes. In the empirical approach the properties of the simulated 'shell-model crystal' are adjusted to give the observed properties by treating the unknown parameters as variables. Figure 2 schematically sketches the possible interactions within a shell-model description. In particular, it is noted that the short-range potentials are specified as acting between different ion shells. As a consequence the actual in-crystal electronic polarizability of the ions becomes dependent on the crystal environment. This is an important physical effect especially for the highly polarizable anions.

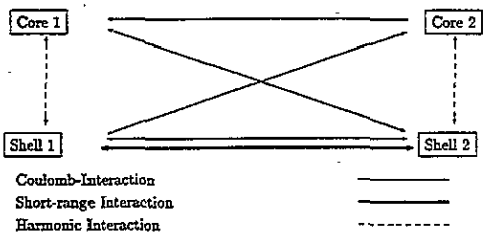

Figure 2. Schematic visualization of all intra- and interionic interactions within a shell-model description of crystals.

The minimization of the lattice energy by independent variation of core and shell coordinates yields the equilibrium configuration of the perfect and the defective lattice. In order to simulate isolated defects a two-region strategy is employed by means of which the crystal is partitioned into two regions. The inner region immediately surrounding the specified defect usually contains ~ 300 ions and is treated atomistically, which means that this region is fully relaxed to its equilibrium structure according to the underlying potentials. The outer region, i.e. the remaining crystal, is described on the basis of the continuum-theoretical Mott–Littleton approximation [6]. The method is coded in the computer program CASCADE [7] which is used in the present investigations. For details of solid-state computer simulations we refer to the monograph edited by Catlow and Mackrodt [8]. All potential parameters appropriate for $BaTiO_3$ and for impurity–oxygen interactions have been taken from the extensive work of Lewis and Catlow [9]. In addition we employed an O^-–O^- pair potential to represent the attractive covalent interaction between the respective O^- hole species [10]. We note that corresponding covalency contributions are absent from the intrinsic O^{2-}–O^{2-} short-range potential. The O^-–O^- potential has been generated by simulations of self-trapped holes in corundum based on the INDO approximation. The self-trapped holes in corundum occurring as V_k-type defects may be considered as negatively ionized hole bipolarons, the derived pair potential is therefore assumed to model as well hole bipolarons in $BaTiO_3$ with sufficient accuracy.

In table 1 we summarize our calculated results of hole-bipolaron formations close to Ti-site and Ba-site acceptor defects. Our simulations suggest that bipolarons may be interpreted

Table 1. Hole-bipolaron formation at Ti-site and Ba-site acceptor defects in $BaTiO_3$.

Acceptor defect	Bipolaronic bond length (Å)	Binding energy (eV) of bipolarons to acceptor-type defects
Al_{Ti}^{3+}	1.24	−1.88
Cr_{Ti}^{3+}	1.23	−0.61
Mg_{Ti}^{2+}	1.24	−1.80
Fe_{Ti}^{2+}	1.22	−0.87
V_{Ti}	1.19	−1.63
Li_{Ba}^{+}	1.21	−0.42
Na_{Ba}^{+}	1.23	+0.03
K_{Ba}^{+}	2.70	+0.80
V_{Ba}	2.57	+0.94

as tightly bound molecules with fixed bond length around 1.2 Å†. This calculated bond length is in satisfactory agreement with the known bond length ~ 1.4 Å of the isoelectronic free F_2 molecules [11]. Regarding trapped bipolarons three different binding energies can be distinguished: the first describes the bonding of bipolarons to acceptor-type defects (corresponding values are compiled in table 1), whereas the second and third measure the affinity of the first and the second hole, respectively, to an acceptor. The latter two binding energies are characterized by the following ionization reactions:

$$1.\ \text{hole ionization: } A\text{–}2O_O^{-1} \longrightarrow A\text{–}O_O^{-1} + O_O^{-1} \tag{3}$$

$$2.\ \text{hole ionization: } A\text{–}O_O^{-1} \longrightarrow A + O_O^{-1}\,. \tag{4}$$

In these equations A denotes an arbitrary acceptor defect, either on a Ba or on a Ti site, A–O_O^{-1} represents an acceptor–hole complex and A–$2O_O^{-1}$, evidently, a hole bipolaron trapped at A. Table 2 summarizes corresponding hole ionization energies for a number of acceptor defects. Resulting from covalency between the O^- ions the 1. hole ionization energy is in all cases greater than the 2. hole ionization energy (negative U behaviour). At this stage two remarks seem to be useful. First, we have assumed that each hole is localized on exactly one oxygen anion. This should be reliable in most situations, however, there is one known example of a V_k-type defect corresponding to a hole trapped at Al_{Ti}^{3+} [12]. This defect centre would therefore require a careful re-examination. In any case however, we believe that the negative U behaviour found so far remains true also in this case. In a forthcoming publication we plan to address all important questions concerning single holes in $BaTiO_3$. Second, it ought to be stressed that our calculated ionization energies include lattice relaxations. They are thus not really comparable with optically induced dissociations possibly observed in photo-ESR experiments, since lattice deformations do not occur during the optical excitation processes. We note, however, that the results of optical shell-model-based calculations (where only the shells are allowed to relax) are in most cases quantitatively unsatisfactory and that thermal simulations (i.e. cores and shells are subject

† We emphasize that an alternative bipolaron formation at exactly one oxygen site (corresponding to a neutral oxygen atom) is not reasonable in the present context. This is true, since in the case of Ti-site acceptors these defects are found to be ~ 1 eV less favourable than the molecular aggregates and, more importantly, they would be paramagnetic: holes would preferably be formed within the twofold-degenerate oxygen 2p orbitals which are oriented perpendicular to the A–O axis. Application of Hund's rules finally yields a spin-triplet ground state. Similarly, we expect a paramagnetic ground state for neutral oxygen atoms hypothetically trapped at Ba-site acceptors. Moreover, corresponding binding energies are generally small.

Table 2. Hole-ionization energies of trapped hole bipolarons in $BaTiO_3$.

Acceptor-type defect	1. hole ionization energy (eV)	2. hole ionization energy (eV)
Ti_{Ti}^{4+} (isolated bipolaron)	1.25	0
Al_{Ti}^{3+}	2.27	0.85
Cr_{Ti}^{3+}	1.29	0.57
Mg_{Ti}^{2+}	2.19	0.82
Fe_{Ti}^{2+}	1.70	0.42
Li_{Ba}^{+}	1.59	0.08
Na_{Ba}^{+}	1.16	0.06

to relaxations) are usually in much better agreement with optical results. This observation might be related to an insufficient representation of the electronic structure by means of shells when taken alone without accompanying lattice relaxations.

The binding of hole bipolarons to Ba-site acceptor-type defects is generally unfavourable, except to small Li-ions. We note that a binding to sodium ions cannot be fully ruled out on the basis of the present simulations, since slight variations of the Na–O short-range potential parameters are able to change the sign of the corresponding binding energy, of which the absolute value is extremely small. The trapping of bipolarons at large Ba-site acceptor defects is particularly unfavourable, because a proper formation of molecules with bond lengths around 1.2 Å is inhibited. Not only K^+-ions but also barium vacancies provide examples for such acceptor defects (see table 1).

Finally, we emphasize that the existence of bipolarons is not only based on the additional covalent O^-–O^- interaction, lattice relaxation aids their formation as well. This could be shown by simulating two holes located on neighbouring oxygen ions without any additional covalent interaction. The holes are bound to each other corresponding to an energy gain of 0.2 eV and to a bond length of 2.69 Å which is slightly less than the perfect lattice separation of 2.80 Å.

2.2. *Embedded cluster calculations*

The shell-model-based simulations described in the preceding section are useful in order to get an overview of the underlying physics. However, further embedded-cluster calculations involving the local electronic defect structure are necessary to correctly model the explicit hole–hole interaction as well as to infer the appropriate spin state of hole bipolarons. Corresponding embedded-cluster calculations have been performed in order to extend the shell-model simulations in the case of Ti-site acceptors. In particular we have considered a Mg^{2+} acceptor impurity cation.

The central quantum defect cluster, see figure 3, consisting of 19 ions besides the O_2^{2-} bipolaron is described by means of effective core potentials [13] implemented on the outer Ba and Ti cations and by a MO *ansatz* for the central acceptor–oxygen complex MgO_6. Gaussian-type basis functions with split-valence (SV) quality have been employed for magnesium [14] and its oxygen ligands [15]; the basis set was further augmented by polarizing d functions. The *ab initio* level of these calculations corresponds to the unrestricted Hartree–Fock (UHF) approximation. In addition, preliminary simulations have been performed including electronic-correlation contributions. These calculations were restricted to single and double electronic excitations (SDCI) with reference to the respective HF states. On the basis of perturbation theory the 20000 energetically most important configurations have been chosen for a diagonalization of the CI-Hamiltonian matrix. With

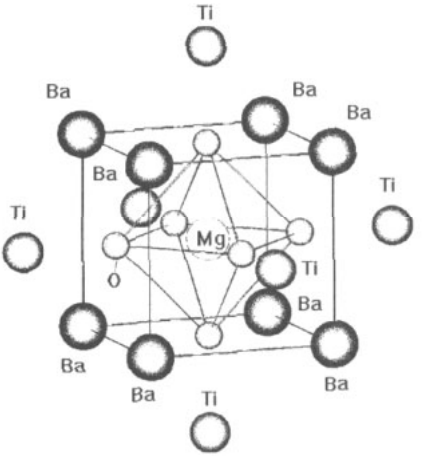

Figure 3. Central quantum defect cluster used throughout the embedded-cluster calculations. The figure assumes all ions on their perfect lattice positions.

this procedure we follow an earlier work of Rawlings and Davidson [16]. We note that simplified SDCI calculations with the excitations being restricted to the oxygen 2p valence shell yielded almost equal results (see below). This is true, since the bonding properties of hole bipolarons localized on oxygen ions near to acceptor-type defects are mainly determined by these orbitals.

The quantum defect cluster has been embedded within a shell-model representation of the outer crystal region. In particular, the known interionic pair potentials are retained in this region. This procedure may be justified by the assumption that explicit defect-induced electronic rearrangements are small in the outer part of the crystal. The total energy of the crystal is minimized with respect to the cluster (nuclear) coordinates R_c and to core and shell coordinates R_o of the outer crystal ions in order to calculate defect energies. The required minimization with respect to the wavefunction Ψ describing the local electronic structure within the cluster region is performed by means of the *ab initio* HF(+CI)–SCF–MO calculations which were introduced above. The relevant energy of the composite system is given by

$$E(\Psi, R_c, R_o) = E_{SM}^{cryst}(R_c, R_o) + E_{QM}^{cl}(\Psi, R_c, R_o) - E_{SM}^{cl}(R_c, R_o). \tag{5}$$

$E_{SM}^{cryst}(R_c, R_o)$ is the shell-model energy of the total crystal and $E_{QM}^{cl}(\Psi, R_c, R_o)$ the quantum-mechanically calculated energy of the defect cluster including the Coulomb interaction between all cluster species (electrons and nuclei) and the outer shell-model ions. $E_{SM}^{cl}(R_c, R_o)$ defines the classical shell-model energy of the cluster. Similar to its quantum-mechanical counterpart this energy includes, besides the intracluster terms, all appropriate cluster–lattice Coulomb interaction energies. The total energy obtained in this way simulates the substitution of a defective shell-model cluster by its quantum-mechanical counterpart. The short-range cluster–lattice interaction is modelled on the basis of the known pair potentials.

In the course of our present work two simplifications have been employed. The first approximation is related to the relaxation of nuclear cluster coordinates: Starting from the CASCADE-equilibrated cluster configuration only the ionic positions of the MgO_6 complex

were slightly adjusted in order to correct for some deficiencies. In each such step the outer lattice was adiabatically equilibrated. Second, we did not require a full multipole consistency between the quantum cluster and its point-charge representation, which is used during the CASCADE step in order to relax the outer lattice corresponding to a specific cluster geometry (see [17] for related information). Instead, we assumed formal ionic charges in the cluster's point-charge representation with holes totally localized on an appropriate number of oxygen ions. At this stage this procedure implies a neglect of bonding charges in particular between the bipolaron partners. We expect, however, that corresponding effects are small, since the cluster's dipole and quadrupole moments calculated on the basis of formal ionic point charges are in reasonable agreement with the respective moments of the quantum cluster. Whereas the dipole moments of the point-charge cluster deviate by about 2% from their quantum analogues, the quadrupole moments are reproduced in the point-charge approximation with differences being slightly less than 6%. The assumed hole-localization properties are further supported by a Mulliken population analysis (MPA). Table 3, for example, presents the MPA ionic charges obtained for the equilibrium bipolaron singlet state employing the HF approximation and lattice relaxation. Although MPA charges should not be taken too seriously, because there is no unambiguous definition of ion charges, the values in table 3 suggest the pronounced degree of hole localization. It is further noted that even in the case of an unrelaxed crystal structure the distribution of two holes over all oxygen ligands turned out to be unfavourable against localization on two adjacent ligands.

Table 3. Ion charges obtained from a MPA for the equilibrium bipolaron singlet state employing the HF approximation and lattice relaxation. O^{2-}_{plane} denotes the oxygen ligands within the plane of the bipolaron O^-–O^- and O^{2-}_{perp} correspondingly the oxygen ions along the axis perpendicular to the bipolaron plane.

Ion	Ionic MPA charge
Mg^{2+}	+1.46
O^{2-}_{plane}	−1.88
O^{2-}_{perp}	−1.89
O^-	−0.95

In our investigations two geometrical hole-acceptor configurations have been considered: the bipolaron with two holes on neighbouring oxygen ions trapped at a magnesium impurity and a linear complex O^-–Mg^{2+}_{Ti}–O^-. These defects have been studied under various conditions.

- Hartree–Fock (HF) treatment of the quantum defect cluster employing a rigid crystal lattice with ions on their perfect lattice positions. Only the O^- partners were allowed to relax.
- HF description of the cluster including complete lattice relaxation.
- The equilibrium lattice of the previous step has been used in further investigations employing a SDCI description of the central defect cluster.

Figure 4 shows our perfect-lattice results. First, we observe that the triplet bipolaron state is energetically more favourable than the singlet state. The reason for this behaviour, which deviates from corresponding results for isolated F_2 molecules, is based on electronic interactions between the O^- ions and crystal ions in the neighbourhood. In particular the triplet bipolaron takes advantage of this interaction because of its antisymmetrical molecular charge distribution. Increasing the bipolaron bond length destabilizes the bipolaron by

increasing delocalization of the holes over all oxygen ligands. This effect is more pronounced in the case of the triplet state. The energetically most favourable configuration, however, corresponds to the linear O^-–Mg_{Ti}^{2+}–O^- complex with localization of the holes on two adjacent oxygen anions. For the purpose of comparison corresponding results have been included in figure 4. The linear configuration is $\sim$ 1 eV more favourable than the triplet state belonging to the bipolaron. Finally, we note that there is no significant energy spacing between the singlet and triplet states of the linear complex.

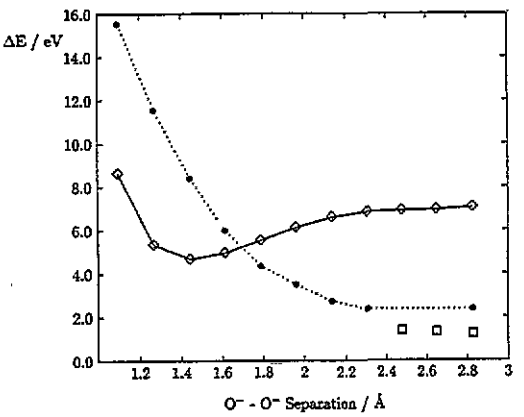

Figure 4. Energy dependence of the bipolaron singlet (◊) and triplet (●) states on the O^-–O^- bond length employing a perfect (thus unrelaxed) crystal lattice and the HF approximation. The additional boxes (□) correspond to the triplet state of the linear defect complex, into which the HF calculations converged in these cases although started with converged (triplet) bipolaron orbitals corresponding to a previous bipolaron configuration.

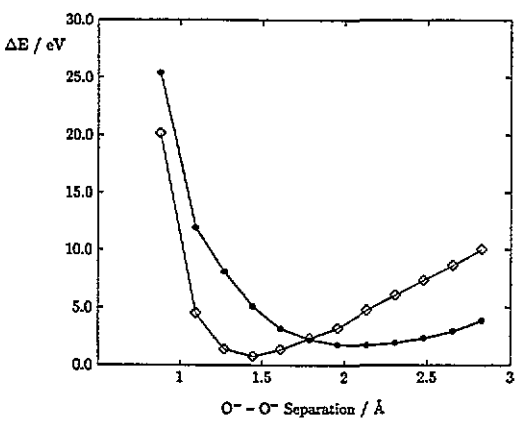

Figure 5. Energy dependence of the bipolaron singlet (◊) and triplet (●) states on the O^-–O^- bond length employing a relaxed crystal lattice and the HF approximation.

Figure 5 displays the energies of the singlet and triplet states of the hole-bipolaron complex employing full lattice relaxation and the HF approximation. In figure 6 the energy

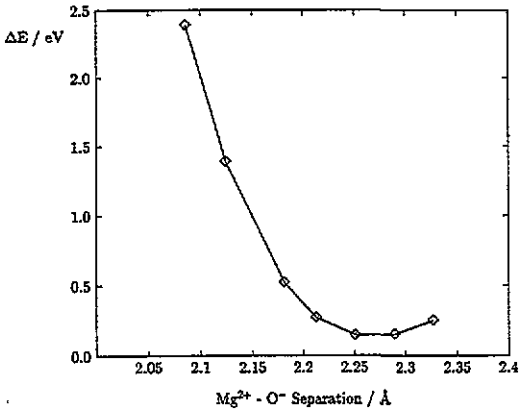

Figure 6. Variation of the bipolaron singlet-state energy as a function of the Mg^{2+}–O^- separation. The shell-model-equilibrated separation corresponds to 2.15 Å.

dependence upon variation of the Mg–O^- separation is shown. The shell-model-based separation of 2.15 Å is by 0.1 Å slightly smaller than the corresponding value obtained from the present embedded-cluster calculations. From figure 5 the equilibrium bipolaron bond length is found to be 1.4 Å, thus also being in good agreement with our shell-model-based simulations. It is further seen that the diamagnetic singlet state is the most favourable electronic state at the equilibrium separation. Increasing the bond length still drops the triplet state below the singlet state. But different from the perfect lattice case the equilibrium singlet state remains by 2 eV more favourable than the lowest triplet state. Again however, within the HF approximation the linear configuration is ~ 0.5 eV more favourable than the alternative bipolaron. Thus, in this approximation the simulated bipolaron represents only metastable defect complex. Our results indicate that neither lattice relaxation nor electronic correlation alone is sufficient in order to favour the bipolaron singlet state against the linear hole-acceptor configuration. It is found that both mechanisms must be operative in order to obtain a diamagnetic bipolaron-type ground state. In this case the singlet state of the bipolaron is 1.67 eV (1.64 eV in the case of SDCI restricted to oxygen 2p electrons) lower in energy than the linear complex. Anticipating at this stage the shell-model-based result that the linear configuration is only slightly bound, the above quoted 1.67 eV roughly measures the bipolaron dissociation energy. From table 2 a corrresponding shell-model value of 2.2 eV is inferred, which is in satisfactory agreement with this estimate. We emphasize that the present CI calculations are based on the HF equilibrium geometries, which may be slightly changed if, instead, CI is consistently employed. It might thus be reasonable to re-examine the energy dependence of the respective bipolaron states as a function of the O^-–O^- separation by consistent inclusion of electronic correlation and lattice relaxation.

2.3. Remarks on high-T_c superconducting oxides

It is tempting in this context to speculate on the possible rôle of small peroxy bipolarons in high-T_c ceramics. In spite of the obvious differences our calculations on formation of such hole bipolarons in $BaTiO_3$ could be of certain interest with regard to hole-pairing mechanisms in high-T_c oxides such as $La_{2-x}Sr_xCuO_4$ and $YBa_2Cu_3O_{7-\delta}$, for instance. Structurally these oxides may be considered as oxygen-deficient perovskites. Up to now the discussion of pairing schemes has been controversial. For example, proposed electron–phonon-mediated mechanisms may be categorized into large- and small-bipolaron schemes.

Whereas Emin and Hillery [18] suggest large bipolarons to be responsible for the observed superconductivity, Mott [19] has recently pointed out that mechanisms involving small hole bipolarons could be realized in these materials. Mott's arguments are to a considerable extent based on the investigations of Alexandrov and Ranninger [20], who have shown that a proper extrapolation of BCS theory to strong electron–phonon couplings leads to pre-existing small bipolarons. In this regime T_c would no longer be given by a dissociation of boson pairs, but rises as a consequence of the Bose–Einstein condensation of the small bipolarons.

It could be possible that small hole bipolarons (i.e. O_2^{2-} peroxy molecules) are formed in high-T_c oxides as a result of electron–lattice coupling and covalent O^-–O^- interactions. Indeed, a preliminary comparison of hole–hole binding energies in $BaTiO_3$ and La_2CuO_4 (corresponding results of which have been taken from [21, 22]) which has been performed on the basis of the same O^-–O^- Morse potential as used in [21] points in this direction: hole bipolarons in $BaTiO_3$ and in La_2CuO_4 (located within CuO_2 planes) are formed corresponding to an energy gain of $\sim$ 0.2 eV in both situations†. However, it seems far from being clear to what extent such small hole bipolarons could be involved in the superconductivity of high-T_c oxides. Several authors have emphasized that a formation of small (bi-)polarons ought to be incompatible with a coherent (i.e. bandlike) motion of these bosons which is necessary for superconductivity to occur (see [18] and references therein). We emphasize that a formation of peroxy bipolarons is accompanied by a pronounced relaxation not only of the surrounding lattice but also of the two O^- partners. Even in the case of small relaxations of the outer lattice (i.e. allowing only major O^- displacements) one would expect rather localized electronic states of the bipolaron related to the important covalency-induced terms, which severely disturb original bandlike hole states. Thus, we may conclude from this qualitative discussion that peroxy hole bipolarons would favour a hopping-type conduction instead of the required coherent motion.

3. Conclusions

In summary, our present calculations support photo-ESR-based speculations favouring diamagnetic hole bipolarons in $BaTiO_3$. Lattice relaxation as well as electronic correlation are important in order to stabilize such defect species in the $BaTiO_3$ crystal lattice against related and competitive linear acceptor-hole complexes. Thus, we have provided necessary conditions for hole bipolarons to exist in this photorefractive material. Probably, these diamagnetic defects are then involved in the light-induced charge-transfer processes observed in $BaTiO_3$. However, in order to prove sufficiency one would have to investigate all diamagnetic crystal defects as a function of all possible crystal compositions. Faced with the vast possibilities for such defects this, however, seems to be an unfeasible task.

Finally, an extrapolation of our results to high-T_c oxides suggests that small peroxy bipolarons are probably not responsible for the observed superconductivity in these materials. However, this qualitatively derived result needs further support by explicit embedded-cluster studies for these high-T_c materials.

† It is noted that this Morse potential is to some extent less attractive than the covalent O^-–O^- potential we have employed throughout our shell-model-based simulations of hole bipolarons in $BaTiO_3$. We have observed that in particular the latter potential is in good agreement with our embedded-cluster studies. However, the Morse potential has been used in the present context in order to give consistency.

Acknowledgments

The financial support of this work by the Deutsche Forschungsgemeinschaft (SFB 225) is gratefully acknowledged. The authors are indebted to Professor O F Schirmer for several helpful discussions.

References

[1] Günter P and Huignard J-P (ed) 1988 *Photorefractive Materials and their Application I and II (Topics in Applied Physics 61 and 62)* (Berlin: Springer)
[2] Fainman Y, Ma J and Lee S H 1993 *Mater. Sci. Rep.* 9 53
[3] Buse K 1993 *J. Opt. Soc. Am.* B **10** 1266
[4] Possenriede E, Jacobs P, Kröse H and Schirmer O F 1992 *Appl. Phys.* A **55** 73
[5] Dick B G and Overhauser A W 1958 *Phys. Rev.* **112** 90
[6] Mott N F and Littleton M J 1938 *Trans. Faraday Soc.* **34** 485
[7] Leslie M 1983 *Solid State Ion.* **8** 243
[8] Catlow C R A and Mackrodt W C (ed) 1982 *Computer Simulation of Solids (Lecture Notes in Physics 166)* (Berlin: Springer)
[9] Lewis G V and Catlow C R A 1986 *J. Phys. Chem. Solids* **47** 89
[10] Jacobs P W and Kotomin E A 1992 *J. Phys.: Condens. Matter* **4** 7531
[11] Herzberg G 1950 *Molecular Spectra and Molecular Structure* vol I (New York: Van Nostrand Reinhold)
[12] Possenriede E 1992 *PhD Thesis* University of Osnabrück
[13] Hay W R and Wadt P J 1985 *J. Chem. Phys.* **82** 270–310
[14] Gordon M S *et al* 1982 *J. Am. Chem. Soc.* **104** 2797
[15] Dunning T H and Hay P J 1977 *Methods of Electronic Structure Theory* ed H F Schaefer III (New York: Plenum) ch 1, pp 1–27
[16] Rawlings D C and Davidson E R 1983 *Chem. Phys. Lett.* **98** 424
[17] Vail J M, Harker A H, Harding J H and Saul P 1984 *J. Phys. C: Solid State Phys.* **17** 3401
[18] Emin D and Hillery M S 1989 *Phys. Rev.* B **36** 6575
[19] Mott N F 1993 *J. Phys.: Condens. Matter* **5** 3487
[20] Alexandrov A S and Ranninger J 1981 *Phys. Rev.* B **23** 1796; 1981 *Phys. Rev.* B **24** 1164; 1992 *Solid State Commun.* **81** 403
[21] Catlow C R A, Tomlinson S M, Islam M S and Leslie M 1988 *J. Phys. C: Solid State Phys.* **21** L1085
[22] Zhang X and Catlow C R A 1991 *J. Mater. Chem.* **1** 233